

LA-UR-13-29265

Approved for public release; distribution is unlimited.

Title: Status of Pu-239 Evaluations

Author(s): Kawano, Toshihiko
Talou, Patrick
Chadwick, Mark B.

Intended for: NEMEA-7/CIELO, International Collaboration on Nuclear Data A workshop
of the Collaborative International Evaluated Library Organisation,
2013-11-05/2013-11-08 (Geel, Belgium)

Issued: 2013-12-06



Disclaimer:

Los Alamos National Laboratory, an affirmative action/equal opportunity employer, is operated by the Los Alamos National Security, LLC for the National Nuclear Security Administration of the U.S. Department of Energy under contract DE-AC52-06NA25396. By approving this article, the publisher recognizes that the U.S. Government retains nonexclusive, royalty-free license to publish or reproduce the published form of this contribution, or to allow others to do so, for U.S. Government purposes.

Los Alamos National Laboratory requests that the publisher identify this article as work performed under the auspices of the U.S. Department of Energy. Los Alamos National Laboratory strongly supports academic freedom and a researcher's right to publish; as an institution, however, the Laboratory does not endorse the viewpoint of a publication or guarantee its technical correctness.

Status of Pu-239 Evaluations

Toshihiko Kawano,* Patrick Talou and Mark B. Chadwick

Los Alamos National Laboratory
Los Alamos, NM 87545, USA

Abstract

This paper summarizes the current status of nuclear data evaluations for n+Pu-239. The nuclear data we address include fission, capture, scattering cross sections, as well as the prompt fission neutron energy spectrum, which have large sensitivities to the criticality benchmark testing. The evaluated nuclear data files currently available for Pu-239 are compared, and the source of differences in the cross sections are discussed. Some open questions on the statistical model calculations for deformed systems are also given.

Introduction

Nuclear reaction data of ^{239}Pu , which is one of the most important major actinides, play an essential role in many nuclear applications, and significant efforts have been devoted to produce a high quality data file that better agrees with both differential and integral measurements available. In this sense the ^{239}Pu file in the nuclear data libraries such as ENDF, JENDL, JEFF, CENDL, and ROSFOND, substantially characterizes the library itself for nuclear energy applications. Therefore knowledge of the details of current nuclear data files provides important information for the development of future international cooperative nuclear data file. In this paper we look into the evaluated ^{239}Pu files in the major nuclear data libraries and discuss the key issues to be resolved in the international file. We take the most recent evaluation of ^{239}Pu in each library, namely CENDL-3.1, ENDF/B-VII.1, JEFF-3.1.2, and JENDL-4.0 unless the release number is explicitly stated otherwise. Since the ^{239}Pu data in ROSFOND is basically the same as JEFF-3.1.2, we drop this library from our comparison.

Summary of Evaluated Files

Here we give a brief summary of each ^{239}Pu file. Since the information given below is basically extracted from the comment section in the files, some ambiguities / errors may exist. The resonance history will be given in a different section.

The file in CENDL-3.1 was carried over from CENDL-2.1 evaluated in 1990. The evaluation based on both experimental data and model calculations with the FUP1 code.

ENDF/B-VII.1 is the same as ENDF/B-VII.0 evaluated in 2006, except for the delayed neutron data. The evaluation is based on ECIS and GNASH calculations. A special care was taken to the $(n,2n)$ cross section, which was evaluated by combining the LANSCE GEANIE prompt gamma-ray measurement and the GNASH calculation. The IAEA standards evaluation for fission cross section was incorporated.

JEFF-3.1.2 is a minor upgrade of JEFF-3.0 that was released in 2006. The actual evaluation year is not given. The evaluation is based on ECIS and GNASH.

JENDL-4.0 is based on the CCONE code calculation in 2007. The simultaneous evaluation was performed for the fission cross section.

Resolved Resonance Region

There are several different resolved resonance parameter sets stored in the files. ENDF adopts the Reich-Moore resonance parameters evaluated by Derrien and Nakagawa, which originally appeared in JENDL-3.2. The resolved resonance region is divided into three energy regions, 0 - 1 keV, 1 - 2 keV, and 2 - 2.5 keV. In CENDL the comment section says the resonance parameters are the same as JENDL-3. However, the energy range is different; the source is unknown. In 2007 the updated parameters, in which the three energy regions were combined into one, were reported by Derrien. JENDL has this resonance parameter set.

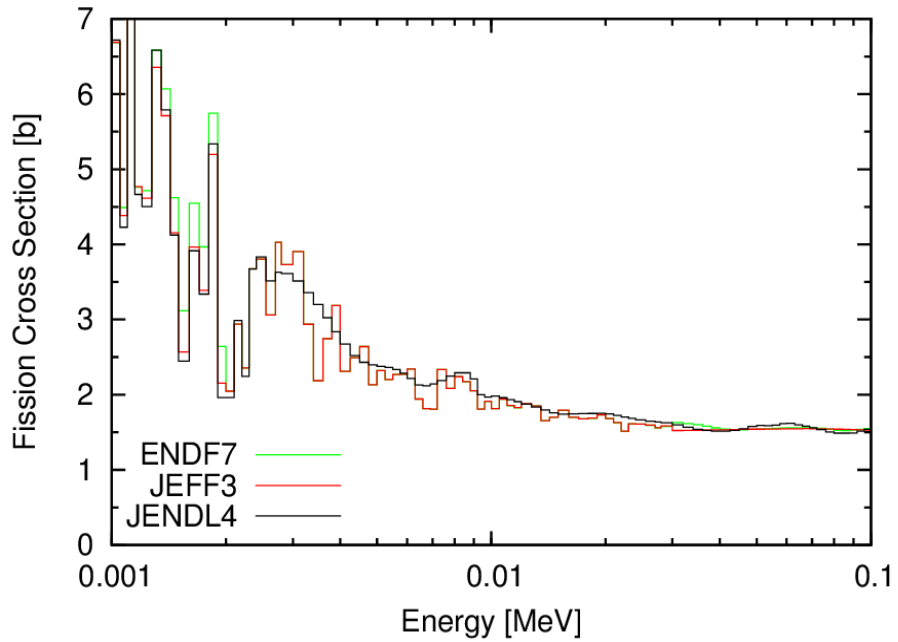
Starting with the resonance parameters in ENDF, JEFF inserted a tiny negative resonance at -0.02 eV for better agreement with some integral benchmark tests. This tweak modifies the slope of fission and capture cross section near the thermal energy, leaving the thermal cross sections unchanged. This effort has been taken over by WPEC/Subgroup 34 “coordinated evaluation of ^{239}Pu in the resonance region” for producing better resonance parameter sets, and benchmark testing of the new parameter set is underway.

Fast Energy Region

Fission Cross Section

The fission cross sections in the fast energy range (above the resolved resonance region) are given by either unresolved resonance parameters in MF=2 (up to 30 keV), or by the point-wise cross section in MF=3. To compare the fission cross sections we first processed the files with NJOY to generate a 640-energy group cross sections in the SAND-II group structure, and they are given in Fig. 1. CENDL is not shown here because it says the unresolved resonance parameters are identical to those in JENDL-3. The ENDF fission cross sections in the 1 - 2 keV region are unexpectedly larger than JENDL and JEFF, despite this is still in the resolved resonance region. This was due to a background cross section given in MF=3. Above 2.5 keV ENDF and JEFF adopt the same unresolved resonance parameters, hence they are identical.

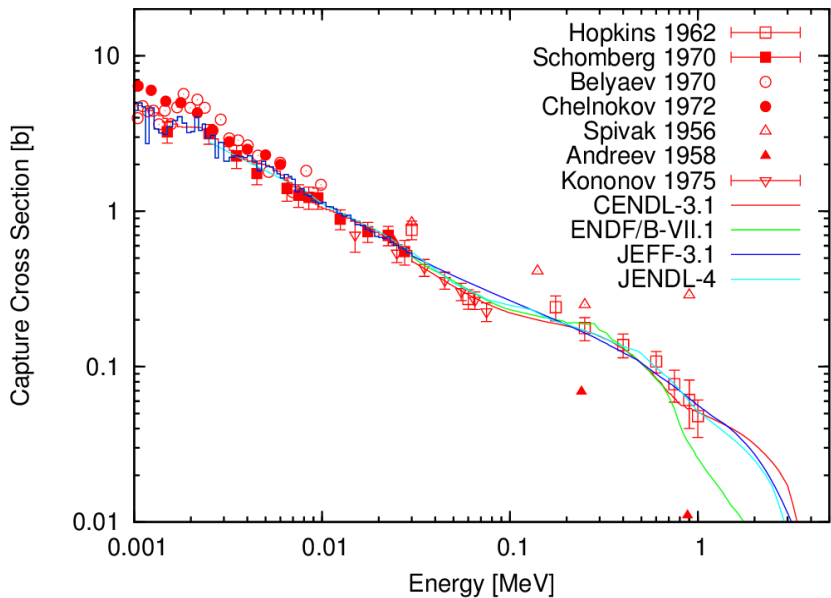
Figure 1: Fission cross sections represented in the 640-energy group structure



Capture Cross Section

Figure 2 compares the evaluated capture cross sections in the fast energy region with some experimental data found in the EXFOR database. The evaluated cross sections agree well up to 20 keV and they start deviating with up to 20% difference around 100 keV. Since the available experimental data are few and scattered, new experiments are needed to fill this gap. With the DANCE detector at LANSCE, LANL measured the capture cross section up to 1 keV, and they will be able to provide new capture data in the higher energy region in near future.

Figure 2: Capture cross sections in the 1 keV to 5MeV range



Inelastic Scattering Cross Section

^{239}Pu has the first excited state at 7.9 keV, and this relatively low threshold energy of inelastic scattering channel competes with the fission and capture reactions in the fast energy range. It is well-known that there are significant differences in the evaluated inelastic scattering cross sections among the nuclear data libraries, although these files work equally well for calculating k_{eff} of Jezebel. This is discussed in the IAEA technical report [1] in detail, and Fig. 3 gives the comparison of the total inelastic scattering cross sections in the different libraries. Since the second excited state energy is 57 keV, and the cross section to the second level is not so large up to 100 keV, the difference in the fast energy range, seen in Fig. 3, is mainly due to the cross section to the first excited state. It is clear that the difference in the inelastic channel is compensated by other nuclear data such as the elastic scattering cross section in the integral benchmark testing.

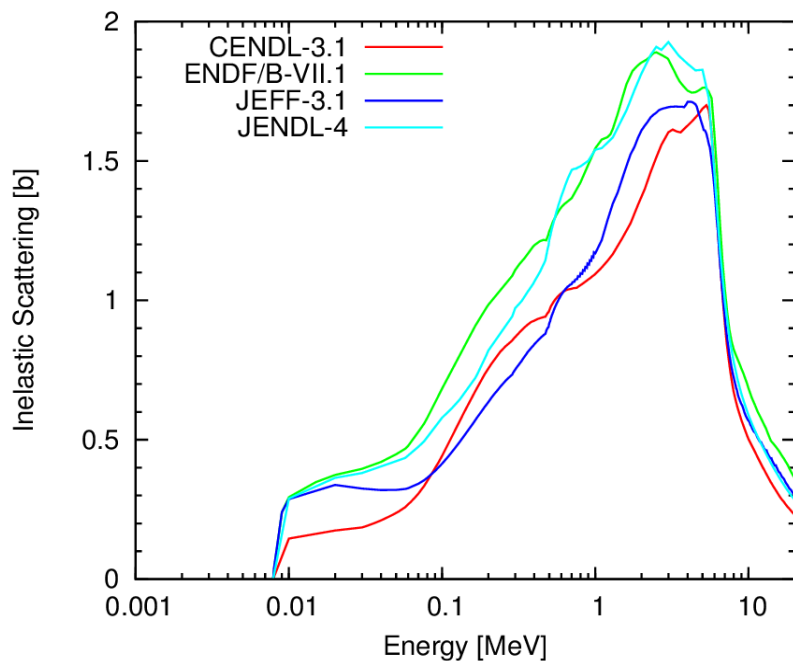
Because there is no direct measurement of the angle-integrated inelastic scattering cross section data, the evaluation of the inelastic scattering relies significantly on the statistical Hauser-Feshbach model calculation, and the following items should be investigated carefully:

- the optical model potential that determines the total compound formation cross section, care must be taken for the coupling scheme as well as the treatment of weakly coupled states,

- the competing channel cross sections (fission and capture), which should be consistent with available experimental data, and
- the width fluctuation model, which re-distributes the total compound formation cross section into individual channels.

We revisited the third item of the width fluctuation by the numerical simulation for the Gaussian Orthogonal Ensemble, and it was confirmed that the current modellings adopted in various Hauser-Feshbach codes do not produce such a large difference in the calculated cross section. We plan to extend this by including the strongly coupled channels.

Figure 3: Comparison of total inelastic scattering cross sections

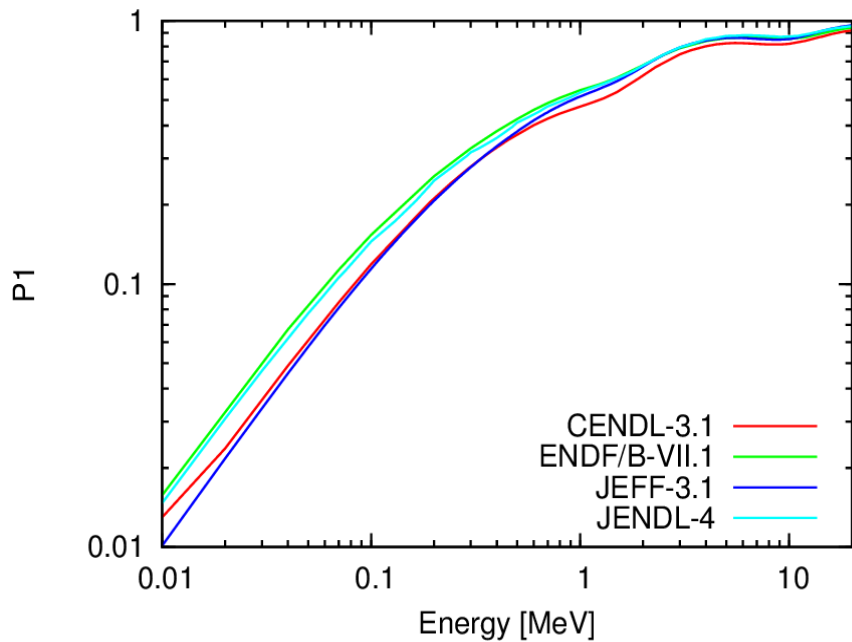


Anisotropy of Elastic Scattering

Radiation transport simulations for the fast neutron systems are sensitive not only to the scattering cross sections but also to the elastic scattering angular distributions, especially for the small systems which have large neutron leakage. The most important nuclear data are the $L=1$ component P_1 for the Legendre expansion of elastic scattering angular distributions. Figure 4 shows the evaluated P_1 in the libraries as a function of incident neutron energies. Since JEFF gives the angular distributions in a tabulated format, we fitted them by the Legendre polynomial. The actual values at 100 keV are: 0.15 for ENDF and JENDL, 0.11 for CENDL and JEFF. This difference is also one of the sources of compensation in calculating k_{eff} of Jezebel.

The scattering angular distribution above the resolved resonance region is solely evaluated by the model calculations, since there is no scattering measurement in this energy region. The model calculation involves both the optical model part that gives the shape elastic scattering, and the statistical model part that gives the compound elastic contribution. The sensitivities of model parameters, as well as the modelling itself such as the number of coupled states, to the calculated anisotropy can be large. For example, it is known that the coupled-channels calculation depends on how many coupled levels are included [2]. We performed simple calculations for ^{239}Pu with CoH_3 and obtained P_1 at 100 keV ranging from 0.12 to 0.18 depending on the number of coupled levels, from 3 to 7. The variation due to the coupling scheme roughly covers the differences among the libraries.

Figure 4: $L=1$ components of elastic scattering angular distributions



Above Fast Energy Region

Fission Cross Section

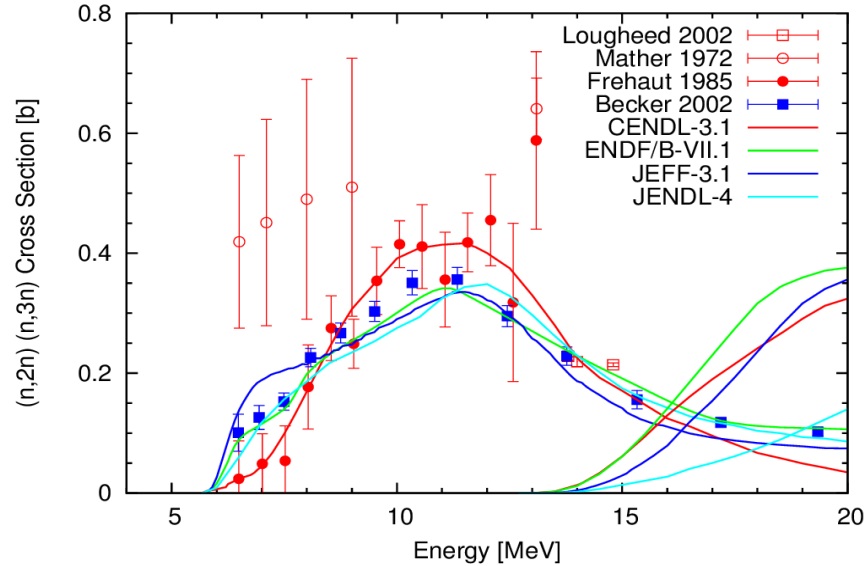
The fission cross sections in the libraries agree within at most 5% above the unresolved resonance range (30 keV). The CENDL, ENDF, and JENDL evaluations are based on the least-squares fitting to the experimental data, so that the difference comes from the selected experiments as well as estimated covariance data. JEFF adopted the Hauser-Feshbach model calculation in which available experimental data were fitted simultaneously.

(n,2n) and (n,3n) Cross Section

Figure 5 shows the comparison of (n,2n) and (n,3n) reaction cross sections in CENDL, ENDF, JEFF, and JENDL. These evaluations are based on both the Hauser-Feshbach calculations and the available experimental data. Note that the experimental data of Frehaut are the original points, not corrected as known.

In this energy region, the elastic scattering cross section is basically equal to the shape elastic scattering calculated with the optical model, and the capture cross section is negligible. Therefore the compound formation cross section is distributed into the multi-chance fission, inelastic scattering, (n,2n), and (n,3n) channels. In this sense these channel cross sections are correlated with each other, and the evaluation should be performed in a consistent way in order to avoid unphysical shape in excitation functions. Even if the fission cross sections are evaluated by the direct fitting to the experimental data, the model calculations are required to reproduce the fission channel to a reasonable extent for evaluating the (n,2n) and (n,3n) channels.

Figure 5: comparison of (n,2n) and (n,3n) reaction cross sections



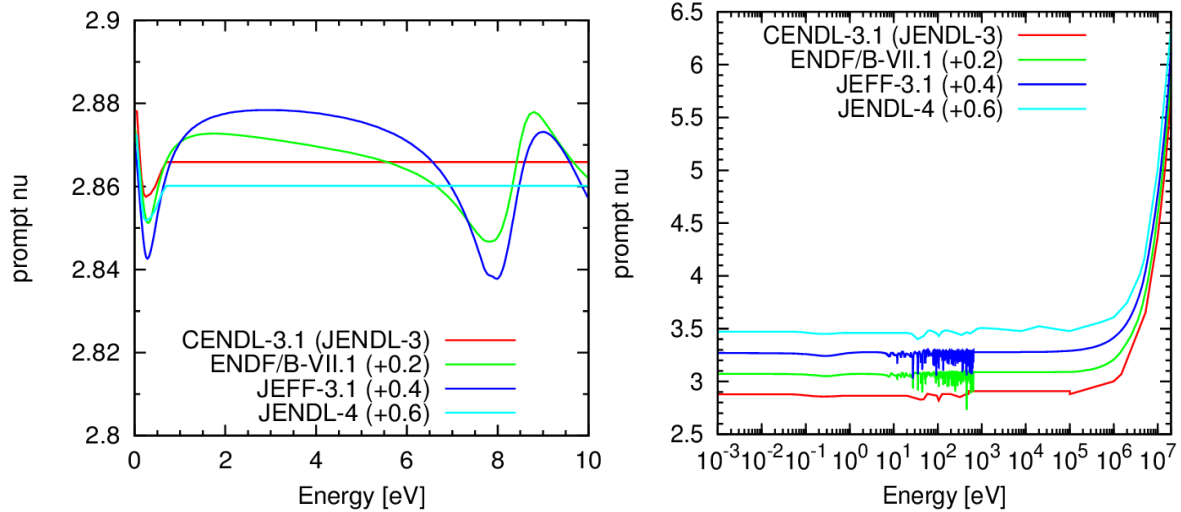
Average Number of Neutrons per Fission

There is a large resolved resonance at 0.3 eV, which modifies the average number of prompt neutrons per fission (v_p). All libraries consider this by representing it in an energy-dependent way. This is shown in Fig. 5. Note that CENDL adopted JENDL-3 v_p . JEFF and ENDF include strong fluctuation in the resolved resonance region, while JENDL-4 smoothed this out. The thermal values in each library are 0.2878 in CENDL (JENDL-3), 2.873 in ENDF, 2.868 in JEFF, and 2.782 in JENDL-4. Because of the dip at 0.3 eV, comparison of the thermal values may also require consideration of the slope in the thermal region, even if the thermal values in the different libraries are consistent with each other.

The thermal values for delayed neutrons in the libraries agree within 5%. JENDL has the low-side value of 0.00622, and JEFF is at the high-side of 0.0065. ENDF is between JENDL and JEFF.

There was a WPEC subgroup 6 “delayed neutron data” where an 8 time-group representation was recommended instead of the traditional 6-group. JEFF is the only library that adopts the 8-group structure for the delayed neutron. All other libraries retained in the 6-group structure.

Figure 5: Average number of prompt fission neutrons per fission as a function of neutron incident energies; left in the eV energy region, and right in the entire energy range. Note that each curve has an offset shown in the figures.



Prompt Fission Neutron Energy Spectrum

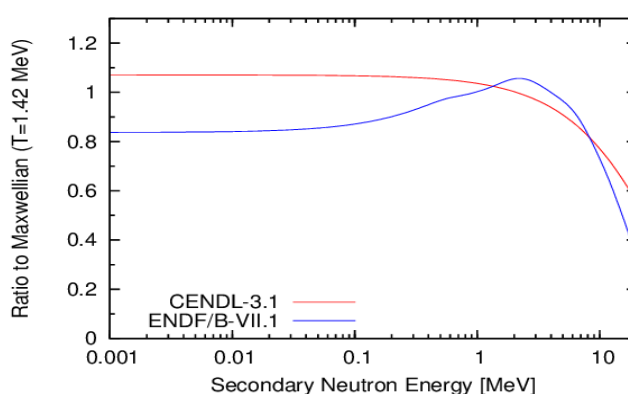
Although the evaluations of prompt fission neutron spectrum for the thermal neutron induced reaction are independent, they are based on the so-called Madland-Nix model (or Los Alamos model). CENDL is an exception - this looks a Maxwellian with the temperature of 1.37 MeV. ENDF, JENDL, and JEFF might have different model parameters together with some modifications to the original Madland-Nix model, the differences among them are surprisingly small and hard to see in a plot. We plot the spectra in ENDF and CENDL only in Fig. 6, which is shown as a ratio to the Maxwellian with the temperature of 1.42 MeV.

Recently WPEC/Subgroup 34 proposed a new set of resolved resonance parameters. They note that indeed these new resonance parameters improve several thermal neutron integral benchmark tests, but we should keep in mind that the calculations of integral quantities also depend on both the prompt fission neutron spectrum and the average number of prompt neutrons at the thermal energy. These quantities are strongly coupled in the neutron transport calculations.

At the higher incident neutron energies, though they are less sensitive to the fission energy applications, different treatments of pre-fission neutron that evaporates from a compound nucleus before scission modify the shape of the spectrum. This calculation involves a complicated exclusive neutron emission calculation in the Hauser-Feshbach model, and only JENDL-4 considers the pre-fission neutrons carefully at this moment. The other libraries include the effect of pre-fission neutrons by correcting the available excitation energy for fission in the residual nucleus. A better modelling for the pre-fission neutron is underway at the IAEA coordinate research project on the prompt fission neutron spectrum, where they plan to re-evaluate the spectrum data for major actinides.

Another important direction of the fission neutron study is the sequential decay of fission fragments by the Monte Carlo technique [3,4]. This methods allows us to calculate not only the neutron energy spectra but also other observables such as prompt gamma-ray energy spectra, number of neutrons as a function of fragment mass, correlation between emitted particles, and so on. The downside of this method is that this requires more detailed description of fission phenomenon, for example the excitation energy shared by two fission fragments and their spin and parity distributions. The Madland-Nix model calculation is still practical for the actual data evaluations. However, the Monte Carlo approach that is fitted to different observables provides us confidence in our fission spectrum modelling.

Figure 6: prompt fission neutron spectra at the thermal energy as a ratio to the Maxwellian of T=1.42 MeV



Conclusion

We have reviewed the evaluated nuclear data of ^{239}Pu in several libraries - CENDL, ENDF, JEFF, and JENDL, and compare them with each other. The comparisons include the cross sections of fission, capture, inelastic scattering, (n,2n), and (n,3n), as well as the elastic scattering angular distribution, the average number of prompt and delayed neutrons, and the prompt fission neutron energy spectrum.

Acknowledgements

This work was carried out under the auspices of the National Nuclear Security Administration of the U.S. Department of Energy at Los Alamos National Laboratory under Contract No. DE-AC52-06NA25396.

References

- [1] A. Plompen, T. Kawano, R. Capote, (2012), "Summary Report on Technical Meeting on Inelastic Scattering and Capture Cross-section Data of Major Actinides in the Fast Neutron Region," INDC(NDS)-0597.
- [2] F. Dietrich, I. Thompson, T. Kawano (2011), "Target-stet dependence of cross sections for reactions on statically deformed nuclei," *Phys. Rev. C*, 85, 044611.
- [3] B. Becker, P. Talou, T. Kawano, Y. Danon, I. Stetcu, (2013), "Monte Carlo Hauser-Feshbach predictions of prompt fission gamma-rays: Application to $n_{th}+^{235}\text{U}$, $n_{th}+^{239}\text{Pu}$, and ^{252}Cf (sf)," *Phys. Rev. C*, 87, 014617.
- [4] R. Vogt, J. Randrup, J. Puet, W. Younes, (2009), "Event-by-event study of prompt neutrons from $^{239}\text{Pu}(n,f)$," *Phys. Rev. C*, 80 044611.